MEMS Sensors for Harsh Environment Applications

Patricia M. Nieva

Department of Mechanical Engineering, University of Waterloo
200 University Ave. W., Waterloo, ON, N2L 3G1, Canada, pnieva@uwaterloo.ca

ABSTRACT

Micro and nano electro mechanical systems (MEMS and NEMS) have emerged as a technology that integrates micro/nano mechanical structures with microelectronics, mainly for sensing and actuation applications. MEMS and NEMS sensor systems that can operate in the presence of high temperatures, corrosive media and/or high radiation will reduce weight, improve machine reliability and reduce cost in strategic market sectors such as automotive, avionics, oil well logging, and nuclear power. We will review recent advances in harsh-environment MEMS and NEMS sensors focusing on devices and materials. Wide-bandgap semiconductor candidates for high temperature (HT) applications will be discussed. The use of Micro-opto mechanical systems (MOEMS) for HT applications will be highlighted.

Keywords: harsh environments, Fabry-Perot, optical microcavity, MEMS, MOEMS, NEMS, NOEMS

1 INTRODUCTION

Silicon-based MEMS technology has enabled the fabrication of a broad range of sensor and actuator systems. These systems are having a great impact in areas that benefit from miniaturization and increased functionality. They have been commercialized for applications such as ink jet printing, crash sensing, and optical projection to name a few. The main advantage of silicon-based technology is the possibility of integration with microelectronics. A great deal of attention is being drawn to the development of integrated MEMS and NEMS to produce smart devices and systems. However, the mechanical and electrical properties of silicon (Si) limit their application in harsh environmental conditions. For example, typical temperatures for automotive and aerospace applications range from 200°C to 600°C. Higher temperatures up to and above 900°C can be found in extremely harsh environments, such as gas turbine engines. When the environment temperature is too high (>180°C), conventional microelectronics suffer from severe performance degradation [1]. Hence, they must reside in cooler areas or be actively cooled. The additional components in the form of longer wires, extra packaging and/or bulky expensive cooling systems, add undesired size and weight to the system. They also require a supply voltage, which is undesirable for HT applications where power source is very limited. Silicon carbide (SiC) [2,3] and group III nitride device technologies [4,6] are promising for operating in harsh environments. In the past decade, tremendous progress has been made in the growth of single crystal SiC wafers and epitaxial growth of crystalline SiC layers on Si and/or SiC wafers [2,10-15]. However, SiC wafers are not (yet) suitable for MEMS and NEMS, as micromachining of these wafers is still a challenge [2-4]. Issues such as high mechanical stress, deposition uniformity and low etch rates need to be tackled before high-quality SiC structural films can be produced [3]. In addition, the affinity of SiC to form carbides and/or silicides by reacting with metals at temperatures above 600°C affect metal contacts degrading the performance of SiC MEMS and NEMS sensors [4]. Furthermore, very little is known about the elastic behavior and long-term stability of SiC micro- and nano-structures at elevated temperatures. Hence, despite the obvious benefits of using SiC for the development of MEMS and NEMS for harsh environments, there are still many hurdles that have to be overcome before it becomes appropriate for manufacturing and can be used reliably in commercial applications [2,3]. Group III nitrides are beneficial as piezoelectric functional components for high temperature operation. For example, Aluminum nitride (AlN) preserves its piezoelectric properties up to 1150°C [5]. However, only a few reports exist about such applications [6]. Remote sensing through optical signal detection has major advantages for safe signal transmission in harsh environments. It is highly resistant to electromagnetic interference (EMI) and radio frequency interference (RFI) and at the same time, it eliminates the need for microelectronics. An economical way to deal with higher temperatures and other aggressive environmental conditions is to build MEMS sensors out of robust materials (e.g. Si, Silicon nitride, SiC) and integrate them with optical signal detection techniques to form MOEMS [7-9]. For instance, Fabry-Perot (FP) microstructures have been used to meet the demand of MEMS sensor systems for harsh environments [7,8]. In this combination, the small and precise size of the sensing elements offers considerable flexibility in choosing the response range and sensitivity of the final sensors. Optical technology has also been used to power a wireless telemetry module for high temperature MEMS sensing and communication [9]. In the following, we review the current status and the main obstacles in wide bandgap semiconductor devices and microsystem components for MEMS and NEMS. We also highlight recent advances in optical MOEMS in the context of using them for harsh environment applications. The use of Fabry-Perot microstructures for the development of a new

MOEMS displacement sensor for high temperature applications is discussed. Simulations and experimental results are presented to show their sensitivity and accuracy.

2 SIC SEMICONDUCTOR DEVICES

SiC is the most mature and the only wide bandgap semiconductor that has silicon dioxide as its native oxide [10]. This allows for the creation of metal oxide semiconductor (MOS) devices. The outstanding mechanical properties and chemical inertness of SiC make it a leading candidate for MEMS and NEMS in a variety of harsh conditions [2,10-15]. Piezoresistive- and capacitive-based sensors are among the most widely used SiC MEMS and NEMS sensing mechanisms.

2.1 Piezoresistive-Based Sensors

The piezoresistive effect in SiC has been used for pressure, force, and acceleration sensors. In general, the piezoresistivity for wide band-gap semiconductors is comparable to that of Si but they can operate at much higher temperatures. However, the contact resistance variation at elevated temperatures can be indistinguishable from the piezoresistance change [14]. In addition, SiC has a relatively low gage factor (30 compared to 90 of Si [11]) which decreases the sensitivity of the sensors as the temperature increases. Okojie et al. [11] developed a piezoresistive pressure transducer which was made of 6H-SiC piezoresistors on a 6H-SiC substrate. The sensor was tested up to 600°C and 200 psi but due to the significant decrease of the gage factor at high temperatures, the output of the transducer required a temperature compensation scheme above 400°C. More recently, Wu et al. [12] developed bulk micromachined pressure sensors for HT applications using polycrystalline and crystalline 3C-SiC piezoresistors grown on a Si substrate. The piezoresistors fabricated from poly-SiC films showed -2.1 as the best gauge factor and exhibited sensitivities up to 20.9-mV/V psi at room temperature. Single-crystalline 3C-SiC piezoresistors exhibited a sensitivity of 177.6-mV/V psi at room temperature and 63.1-mV/V psi at 400°C. Their estimated longitudinal gauge factor along the [100] direction was estimated at about -18 at room temperature but dropped to -7 at 400°C. Atwell et al. [13] developed a bulk-micromachined 6H-SiC piezoresistive accelerometer for impact applications. The accelerometer was tested up to 40,000g. Sensitivities ranging from 50 to 343 nV/g were measured for differing sensing elements but non-linear behavior was observed over the shock range relative to a commercial accelerometer (with sensitivity of 1.5μV/g).

2.2 Capacitive-Based Sensors

Capacitive-based sensors have also been used to sense pressure, force, acceleration, and flow rate. They are attractive for HT applications because the device performance is not susceptible to contact resistance variations but they exhibit performance degradation due to the wiring parasitic capacitances and test setup. SiC capacitive sensors are mainly used for pressure sensing and they are mainly fabricated using bulk-micromachining techniques. Young et al. [14] developed a single crystal 3C-SiC capacitive pressure sensor fabricated on a silicon substrate. The sensor demonstrated sensing capabilities up to 400°C and was tolerant of contact resistance variations. However, it exhibited different responses at different temperatures of operation, which was attributed to trapped air inside the cavity and thermal mismatch. A promising approach to pressure sensing in corrosive environments was developed by Pakula et al. [15] using post-processing surface micromachining. The sensing membrane was fabricated in low-stress PECVD SiC. To avoid problems related with wiring parasitic capacitances, the sensor was integrated monolithically to a CMOS readout circuit. The sensor showed stable behavior from 10mbar up to 5bar.

3 OPTICAL MEMS SENSORS

Optical MEMS sensors are highly adaptable to harsh environments, can measure displacement, pressure, temperature and stress, can be easily incorporated into sensor arrays by using multiplexing methods, and are suitable for liquid and gas measurements. However, simpler processing techniques and therefore lower manufacturing costs are desirable. Moreover, simplification of the sensing elements and the fabrication process will be helpful for their mass production and commercialization. Fiber-Optic MEMS and MOEMS sensors are lately being developed for harsh environmental conditions.

3.1 Fiber-Optic MEMS Sensors

Fiber-optic MEMS are robust, highly resistant to EMI and RFI, and can potentially detect displacements on a sub-nanometer scale. However, their performance depends on mechanical–thermal noise, photodetector noise, fabrication imperfections and assembly. Eklund and Shkel [16] demonstrated that the finesse of a Fiber Optic Fabry-Perot MEMS can decrease up to one order of magnitude due to surface roughness, curvature or a slight deviation from parallelism, thus greatly reducing the resolution of the sensor. Xiao-qi et al. [17] developed a fiber-optic MEMS pressure sensor for harsh environments based on Fabry–Perot interferometry. A dual-wavelength demodulation method was used to interrogate the sensor and results show that the sensor has reasonable linearity and sensitivity within 0.1 MPa to 3 MPa. However, the fabrication is complicated and the sensor and the fibre must be well aligned to avoid the increase of the signal-to-noise ratio due to instability of the reflected signal.

3.2 MOEMS Sensors

Fabry-Perot Interferometric techniques can be easily applied to membranes or cantilevers that, if fabricated with robust materials, can be utilized to develop contact-free sensor components with high sturdiness in harsh conditions. Compared to sensors that utilize optical fibers or multi-chip structures [16,17], single-chip Fabry-Perot MOEMS sensors do not require alignment or sophisticated optical stabilization techniques [7,8,18]. In contrast to cumbersome and ambiguous fringe-counting optical detection schemes associated with large cavity FP sensors used in the literature, the small cavity length of these sensor (2-3µm) allows small intensity shifts to be uniquely related to the relative displacement of the moving mirror. Haueis et al. [8] developed a Si-based resonant force sensor packaged with fiber-optic signal detection for high temperature operation. An off-chip capacitive detection system was also used to verify the operation of the sensor up to 175°C. The optical detection showed a resolution of the resonator deflection to be more than ten times better than the capacitive detection. Wang et al. [18] developed a new Fabry-Perot pressure microsensor which has been successfully tested up to 30psi and 120°C. However, because of the bridge configuration of the sensor, a corrugated diaphragm was used to alleviate both, the signal averaging effect and the cross-sensitivity to temperature.

4 FABRY-PEROT MOEMS SENSOR FOR HIGH TEMPERATURE APPLICATIONS

We have developed the Fabry-Perot MOEMS displacement sensor (FPMOD) shown in Fig. 1 that is suitable for high temperature applications and can be easily integrated with standard Si micromachining.

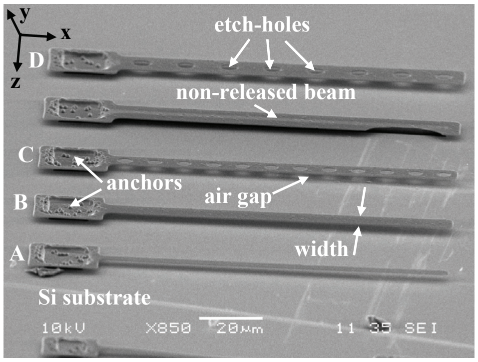

Figure 1: Fabry-Perot MOEMS displacement sensors with a fundamental resonant frequency of ~ 45 kHz [7]

Beam Type	Length (µm)	Width (µm)	Etch-Hole diameter (µm)	Air Gap @ spot (µm)	Spot Location (µm)
A	122.5	4.25	-	2.84	5
B	119.6	8.17	-	2.66	17.5
C	123.5	9.31	3.92	2.60	17.5
D	118.5	13.39	5.56	2.62	22.5

Table 1: Summary of measured parameters for the Fabry-Perot MOEMS displacement sensors shown in Fig. 1

A cantilever beam fabricated in low-stress LPCVD silicon nitride) forms the top mirror for the Fabry-Perot interferometer while the silicon substrate below provides the bottom mirror. These two mirrors form an optical microcavity for a monochromatic laser beam incident at the top. For this cavity arrangement, the total interferometric light back-reflected depends on the height of the optical microcavity at the location where the laser beam is directed (spot). When the substrate vibrates, there is a relative deflection of the beam with respect to the substrate and hence a change in the microcavity height. The amplitude of the substrate motion can be calculated by measuring the back-reflected light. Cantilever beams have advantages over bridge structures because the lowest natural frequency is 16% of a bridge with the same dimensions, allowing measurement of lower frequencies. Also residual stresses do not significantly affect the resonant frequency of cantilevers [19], but do change the resonant frequency of a bridge operating at high temperatures [20]. In addition, they eliminate problems due to stress-stiffening effects and variation of the optical path length due to coupled photo-elastic and thermal-optical effects, all of which are critical to the successful realization of sensors for high temperature applications. To the best of our knowledge this FPMOD sensor is the first device in the literature that employs a single layer cantilevered structure together with a new extrinsic intensity-modulated optical interrogation method.

4.1 Frequency Response

The modeling and details of the experimental setup used for the determination of the frequency response of the FPMOD sensors were described in Ref. [7]. The measured frequency responses shown in Fig. 3 are for the set of sensors included in Table 1 to which a 10nm amplitude harmonic excitation was applied. These devices were tested at atmospheric pressure (14.7psi) and room temperature (23°C). Their fundamental frequencies are 43.5 ± 3 kHz and their total viscous damping factor (ζ_1 , mode 1) vary from 0.19 to 0.3.

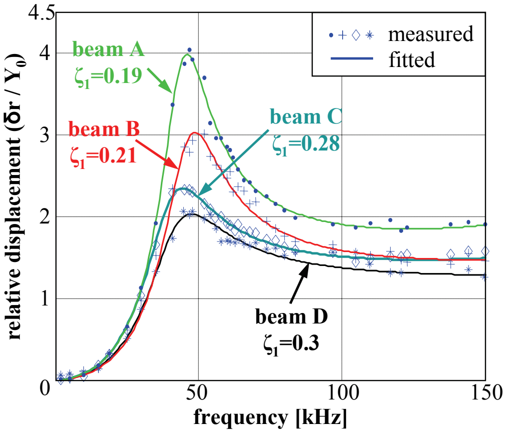

Figure 2: Measured and fitted frequency response for all FPMOD sensors listed in Table 1 [7]

4.2 Temperature Dependence

The mechanisms leading to temperature dependence of the FPMOD frequency response are mainly due to (1) shift of the resonant frequency arising from the variation of the Young's modulus, density and coefficient of thermal expansion of the Si_xN_y film (2) variation of the take-off angle of the beam curling due to induced uniform stress (3) variation of the viscous damping coefficient due to variation of the density and the viscosity of the air, and (4) changes of the optical path lengths due to the coupled thermal-optical and photo-elastic effects. For the FPMOD type A depicted in Fig. 1, a variation of temperature from $23°\mathrm{C}$ to $600°\mathrm{C}$ causes a drift in the fundamental resonant frequency of about 5.1%, which is much less than the 20% drift reported for bridges in Ref. [20]. For the same FPMOD, the take-off angle is $\sim 5.7\mathrm{mrad}$. Neglecting the effects of stress gradients, the same temperature change produces a variation in the take-off angle of $-0.38\mathrm{mrad}$. This variant decreases the air gap height at the spot location by about $43\mathrm{nm}$ moving the point of operation of the sensor about 1.3% and hence, decreasing the sensor's optical sensitivity [7]. However, if the temperature of operation of the sensor is known, both these effects can be corrected for.

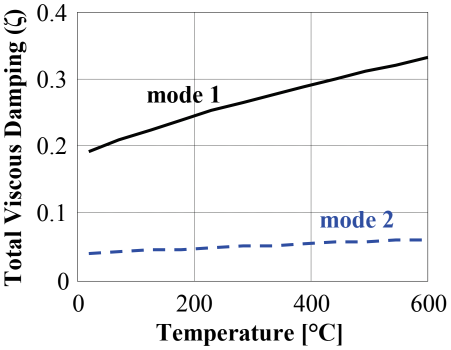

Figure 3: Calculated temperature dependence of the total air viscous damping coefficient (n = 1,2) for FPMOD type A

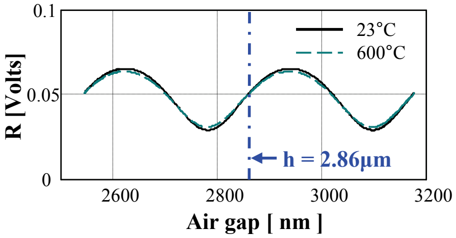

Figure 4: Shift of the optical transfer function of the FPMOD type A due to the temperature dependence of the optical path length.

Another mechanism that leads to sensor temperature dependence is the air viscous damping which depends on the viscosity and the density of the air, both of which are dependent on temperature. Fig. 3 shows the variation of the air viscous damping as a function of temperature for the FPMOD type A for the first two modes of vibration and at atmospheric pressure. It can be seen that the variation in viscous damping for a temperature varying from $23°\mathrm{C}$ to $600°\mathrm{C}$ is ~ 0.14. This corresponds to a decrease in relative displacement of ~2 and hence, a decrease of sensor sensitivity around the fundamental resonant frequency. Finally, a variation of temperature from $23°\mathrm{C}$ to $600°\mathrm{C}$ corresponds to a small variation of the optical path length (around $2.27\mathrm{nm}$) due to the coupled thermal-optical and photo-elastic effects. Fig. 4 shows that the effect of the temperature is less significant if the point of operation is close to the point of maximum sensitivity [7].

5 CONCLUSIONS

We have reviewed recent advances in MEMS sensors for harsh-environments focusing on fabricated devices. SiC is an excellent candidate for the development of MEMS and NEMS for harsh environments but there are still many hurdles that have to be overcome before it becomes appropriate for manufacturing and can be used reliably in commercial applications. The adaptability, resistance to EMI and RFI and high sensitivity make MOEMS sensors ideal for applications in harsh environments. Much progress has been made in the development of simpler processing techniques and simplification of MEMS sensing elements. A new Fabry-Perot MOEMS displacement sensor for HT applications was presented. Results show very small influence of high temperatures on the sensitivity of this sensor. The simple configuration of the optical detection system makes it ideal for integration in the sensor package.

REFERENCES

[1] J. Goetz, "Sensors that can take the heat," Sensors Magazine, 20-38, June 2000
[2] M. Mehregany, X. Fu and L. Chen, NSTI-Nanotech 2006, 3, 471-474, 2006
[3] D. Gao, M. Wijesundara, C. Carraro, R. Howe and R. Maboudian (2004), IEEE Sensors Journal 4(4):441-448.
[4] R. C. Turner, P.A. Fuierer, R.E. Newnham and T. R. Shrout, Applied Acoustics, 41, 299-324, 1994
[5] C. Jacob, P. Pirouz, H. I. Kuo and M. Mehregany, Solid State Electronics, 42(12), 2329-2334, 1998
[6] D. Doppalapudi, R. Mlcak, J. Chan, H. Tuller, J. Abell, W. Li and T. Moustakas, Electrochem. Soc. Proc., 6, 287-299, 2004
[7] P. Nieva, N. McGruer and G. Adams, J. Micromech. Microeng., 16, 2618-2631, 2006
[8] M. Haueis, J. Dual, C. Cavalloni, M. Gnielka, and R. Buser, J. Micromechanics and Microengineering, 11:514-521, 2001
[9] M. Suster, W. Ko and D. Young, J. Microelectromech. Systems, 13(3), 536-541, 2004
[10] S. Dakshinamurthy, N. R. Quick and A. Kar, J. Phys. D: Appl. Phys., 353 - 360, 2007
[11] R. Okojie, G. Beheim, G. Saad and E. Savrun, AIAA Space 2001 Conference and Exposition, Albuquerque, NM, 1-8, 2001
[12] C. Wu, C. Zorman and M. Mehregany, IEEE Sensors Journal, 6 (2), 316-324, 2006
[13] A. Atwell, R. Okojie, K. Kornegay, S. Roberson and A. Beliveau, Sensors and Actuators A, 104, 11-18, 2003
[14] D. J. Young, J. Du, C. Zorman and W. Ko, IEEE Sensors Journal, 4, 464-470, 2004
[15] L. Pakula, H. Yang, H. Pham, P. French and P. Sarro, J. Micromech. Microeng. 14, 1478-1483, 2004
[16] E. Eklund and A. Shkel, J. Micromech. Microeng., 15, 1770-1776, 2005
[17] N. Xiao-qi, W. Ming, C. Xu-xing, G. Yi-xian and R. Hua, Meas. Sci. Technol. 17, 2401–2404, 2006
[18] W. Wang, R. Lin, D. Guo and T. Sun, Sensors and Actuators A, 116, 59-65, 2004
[19] R. A. Buser and N. F. De Rooij, Sensors and Actuators A, 17, 145-54, 1989
[20] M. Fonseca, J. English, M. von Arx and M. Allen, J. Microelectromech. Syst., 11, 337-43, 2002